Plant Communications, Volume *2*

Supplemental information

A *Phelipanche ramosa* KAI2 protein perceives strigolactones and isothiocyanates enzymatically

Alexandre de Saint Germain, Anse Jacobs, Guillaume Brun, Jean-Bernard Pouvreau, Lukas Braem, David Cornu, Guillaume Clavé, Emmanuelle Baudu, Vincent Steinmetz, Vincent Servajean, Susann Wicke, Kris Gevaert, Philippe Simier, Sofie Goormachtig, Philippe Delavault, and François-Didier Boyer

Supplementary Figures and Tables

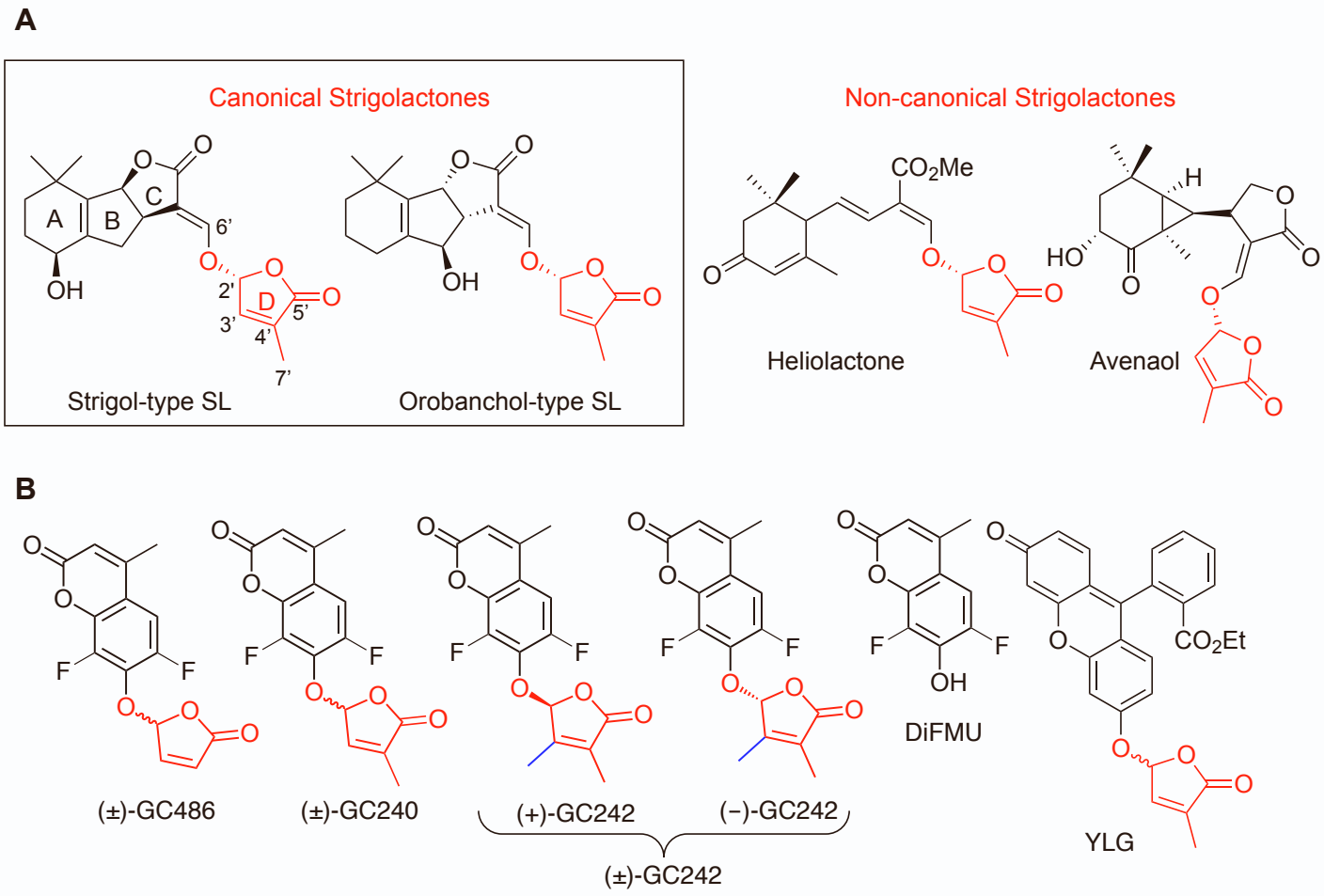

Supplementary Figure 1. Chemical structures. (A) Natural strigolactones. **(B)** Profluorescent probes. GC series and Yoshimulactone (YLG).

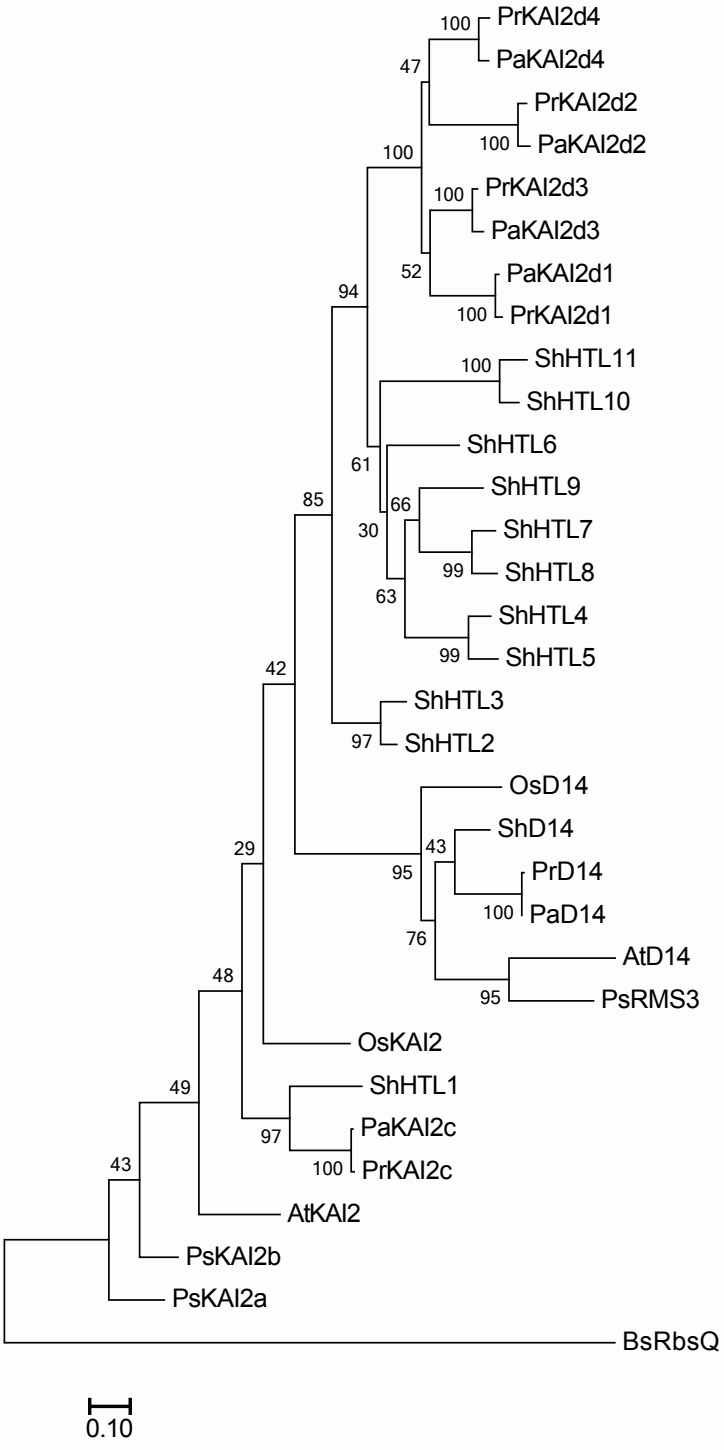

Supplementary Figure 2. Phylogenetic analysis of KAI2 and D14 nucleotide sequences. The phylogenetic tree was constructed with the maximum likelihood method and 1,000 bootstraps replicates by means of RAxML. Scale bar = 0.1 substitutions per site.

Data file S1. D14 and KAI2 amino acid sequences
Data file S2. D14 and KAI2 nucleotide sequences
Data file S3. MAFFT alignement of D14 and KAI2 amino acid sequences
Data file S4. MAFFT alignement of D14 and KAI2 nucleotide sequences
Data file S5. Trimmed MAFFT alignement of D14 and KAI2 amino acid sequences
Data file S6. Trimmed MAFFT alignement of D14 and KAI2 nucleotide sequences

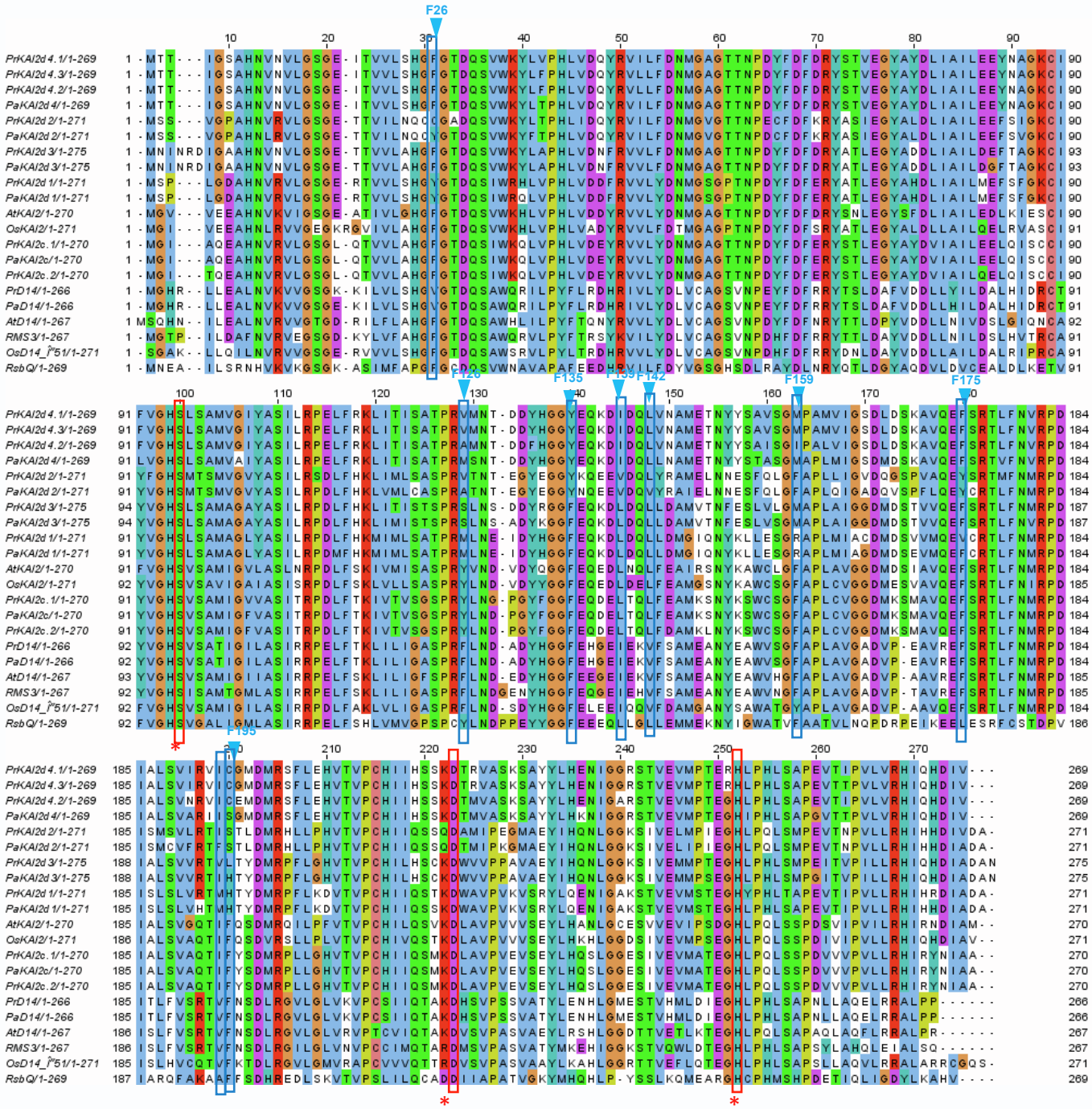

Supplementary Figure 3. Sequence alignment of *Phelipanche ramosa* (*Pr*) and *P. aegyptiaca* (*Pa*) KAI2 protein with D14 and KAI2 proteins from *Arabidopsis* (At), rice (Os), pea (RMS), and the bacterial RbsQ. The three amino acid residues corresponding to the catalytic triad are marked with asterisks. Amino residues highlighted in the Figure 1**B** are indicated with a blue arrowhead. Amino acid numbers are indicated for AtD14. Note that the rice OsD14 protein has a non-conserved 50-amino-acid N-terminal extension omitted in the alignment.

A

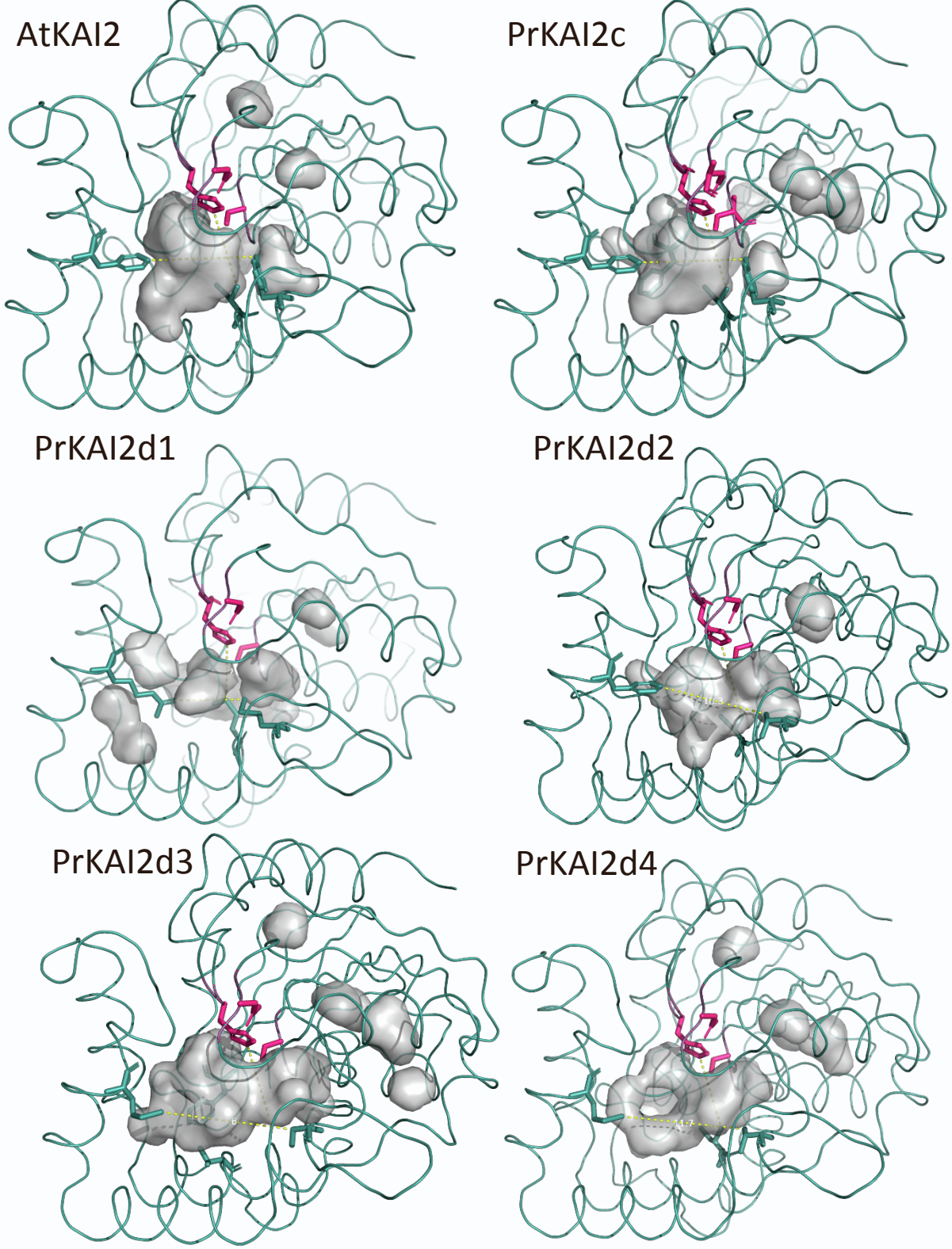

B

Protein	Distance position 124-157 (Å)	Distance position 246-193 (Å)
AtKAI2	10.643	7.693
PrKAI2c	9.996	7.619
PrKAI2d1	6.612	6.168
PrKAI2d2	10.269	7.649
PrKAI2d3	11.598	7.468
PrKAI2d4	11.658	7.637

Supplementary Figure 4. Models of the ligand pockets of the *P. ramosa* KAI2 proteins. (A) Visual representation (different from Figure 1c) of the ligand pockets of the *P. ramosa* KAI2 proteins. The KAI2 protein sequences were modeled with the chain A of the karrikin-bound *Arabidopsis* KAI2 structure as a template (PDB: 4JYP). The protein structures were generated with PYMOL and the cavities within the homology models were visualized with the surface mode on the setting “cavities and pockets culled” within PYMOL. The sticks represent parts of the catalytic triad (Ser, His, Asp). **(B)** Width/length of the ligand pockets of the *P. ramosa* KAI2 proteins.

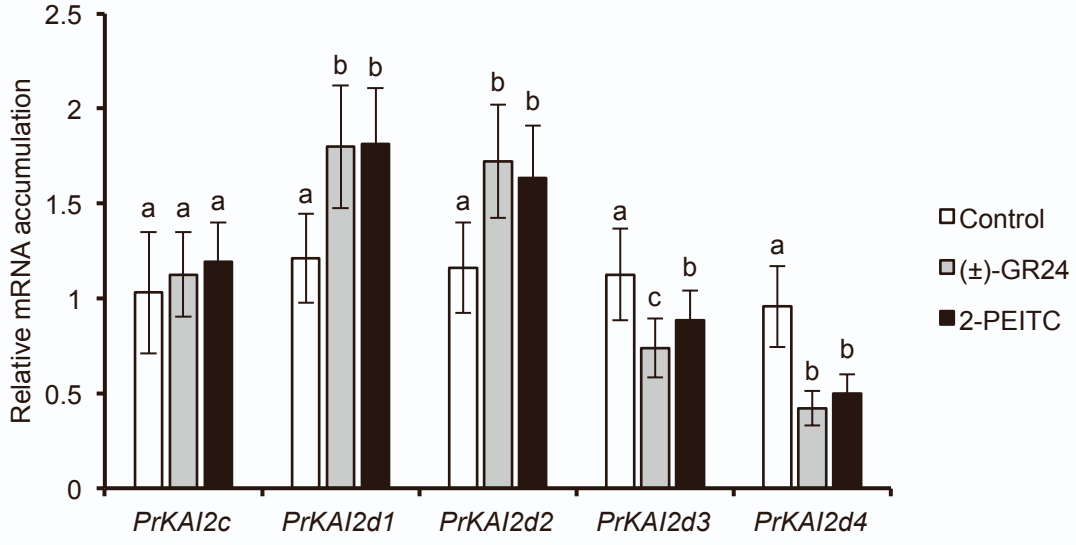

Supplementary Figure 5. Expression of the KAI2 genes in *P. ramosa*. RNA was isolated from seeds conditioned for 7 d, and seeds treated for 6 h with mock (control) or 0.1 µM of the indicated stimulant. *EF1-α* was used as the reference gene, and expression in mock- and stimulant-treated seeds was normalized to gene expression in seeds conditioned for 7 d (ΔΔCt). Data are means ± standard error (n = 3). Letters indicate significant differences in expression between conditions ($P < 0.001$, Tukey-HSD test).

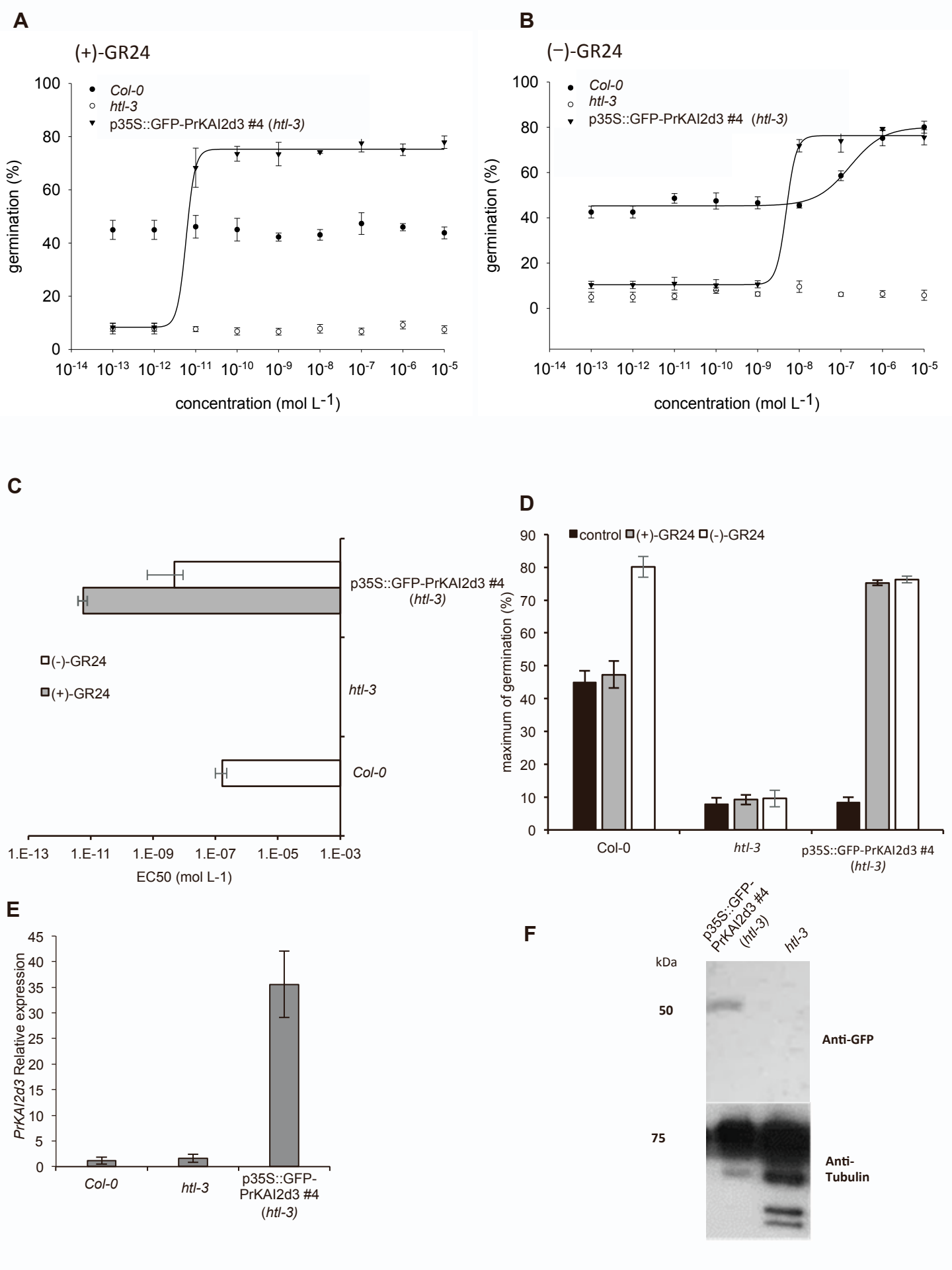
A
(+)-GR24
Col-0
htl-3
p35S::GFP-PrKAI2d3 #4 (htl-3)
germination (%)
concentration (mol L-1)
B
(−)-GR24
Col-0
htl-3
p35S::GFP-PrKAI2d3 #4 (htl-3)
germination (%)
concentration (mol L-1)
C
p35S::GFP-PrKAI2d3 #4 (htl-3)
(-)-GR24
(+)-GR24
htl-3
Col-0
EC50 (mol L-1)
D
control
(+)-GR24
(-)-GR24
maximum of germination (%)
Col-0
htl-3
p35S::GFP-PrKAI2d3 #4 (htl-3)
E
PrKAI2d3 Relative expression
Col-0
htl-3
p35S::GFP-PrKAI2d3 #4 (htl-3)
F
p35S::GFP-PrKAI2d3 #4 (htl-3)
htl-3
kDa
50
75
Anti-GFP
Anti-Tubulin

Supplementary Figure 6. Dose response germination stimulant activities of (+)-GR24 and (−)-GR24 with *Arabidopsis* lines. Dose response germination stimulation activities and modeled curves of (+)-GR24 **(A)** and (−)-GR24 **(B)** on seeds of *Arabidopsis* Col-0 and *htl-3*/p35S::PrKAI2d3. **(C)** Half maximal effective concentration (EC_{50}). **(D)** Maximum germination stimulation activities. Data are indicated ± SE. **(E)** Relative accumulation of *PrKAI2d3* transcripts in *Arabidopsis* Col-0, *htl-3,* and p35S::GFP-PrKAI2d3 #4 (*htl-3*) seeds imbibed for 24 h. **(F)** Accumulation of PrKAI2d3 proteins in *Arabidopsis* p35S::GFP-PrKAI2d3 #4 (*htl-3*) and *htl-3* 5d-old seedlings.

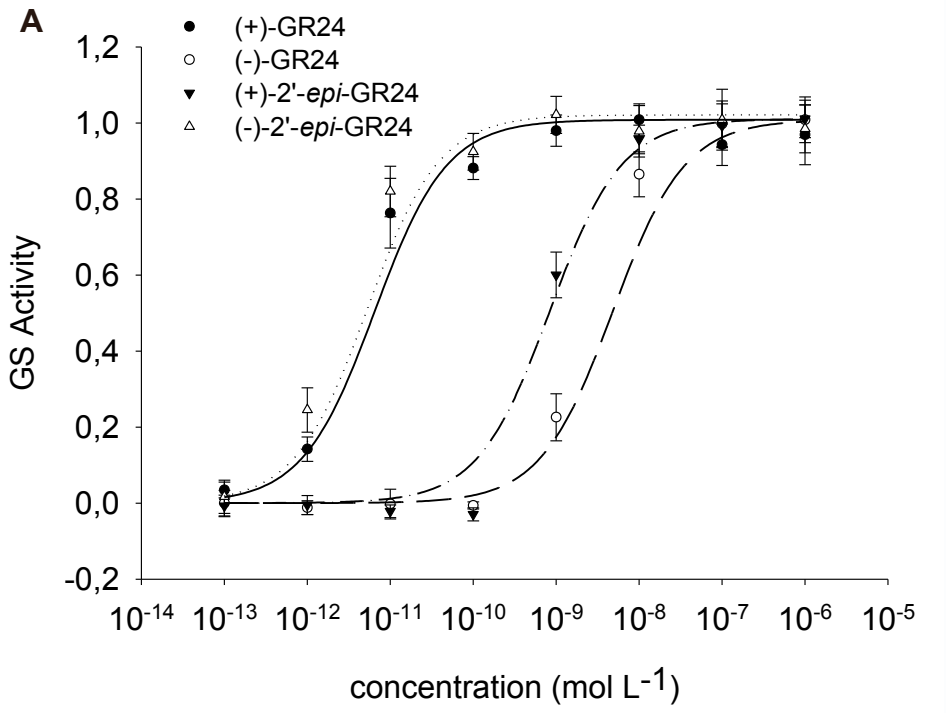

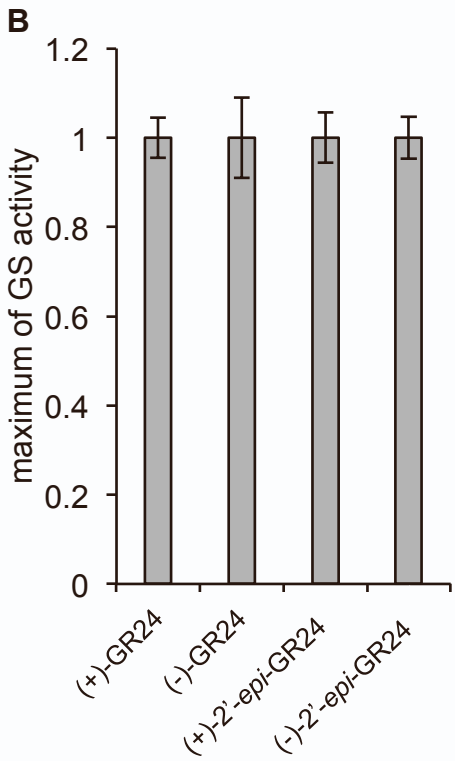

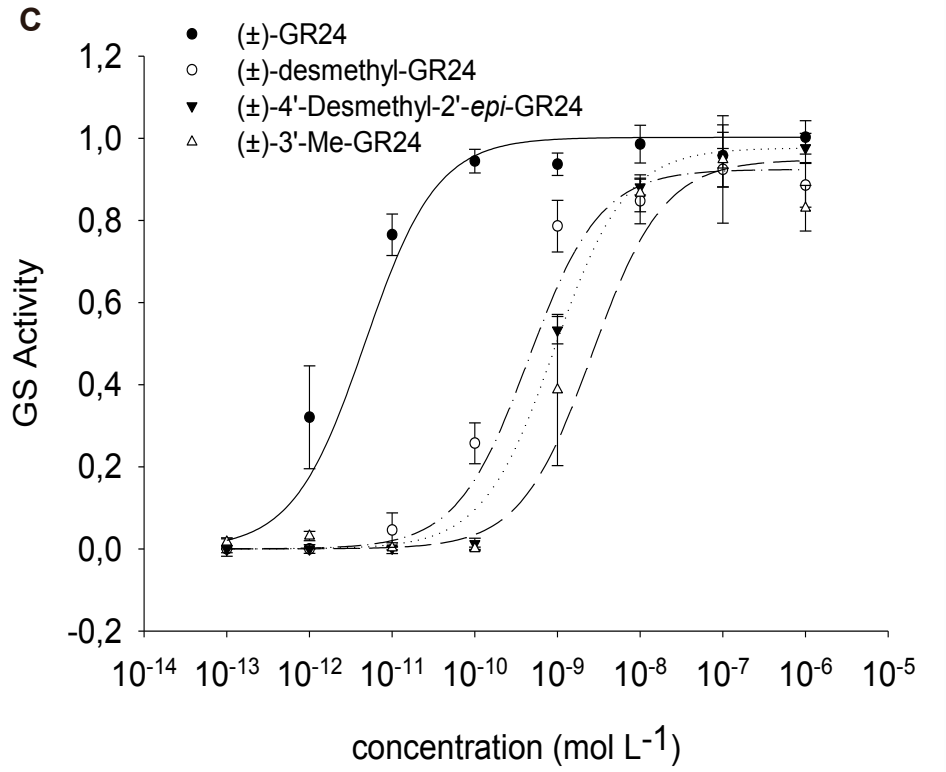

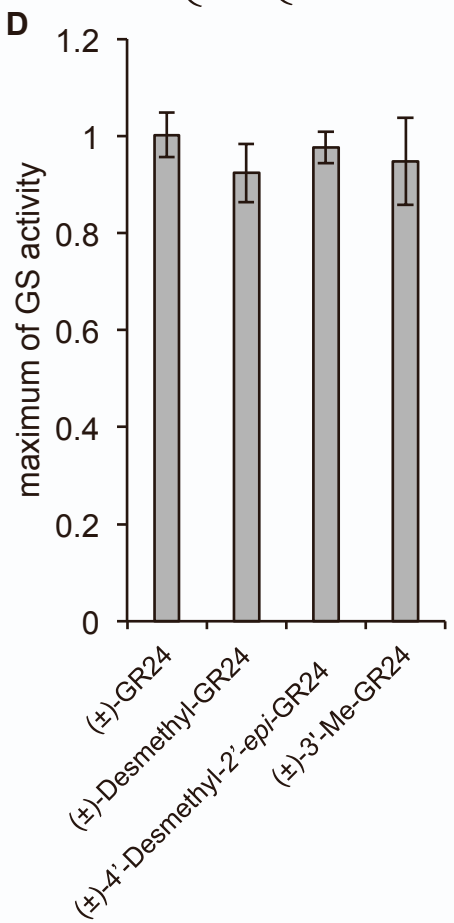

Supplementary Figure 7. Germination assay on *P. ramosa* parasitic-plant seeds of GR24 isomers [(+)-GR24, (−)-GR24, (+)-2'-*epi*-GR24, and (−)-2'-*epi*-GR24] and methyl variation on the GR24 D-ring [(±)-Desmethyl-GR24, (±)-4'-Desmethyl-2'-epi-GR24, and (±)-3'-Me-GR24]. **(A**) and **(C)** Dose response germination stimulation activities and modeled curves.**(B)** and (**D)** Maximum germination stimulation activity relative to (±)-GR24 (1 µM). Data are indicated ± SE.

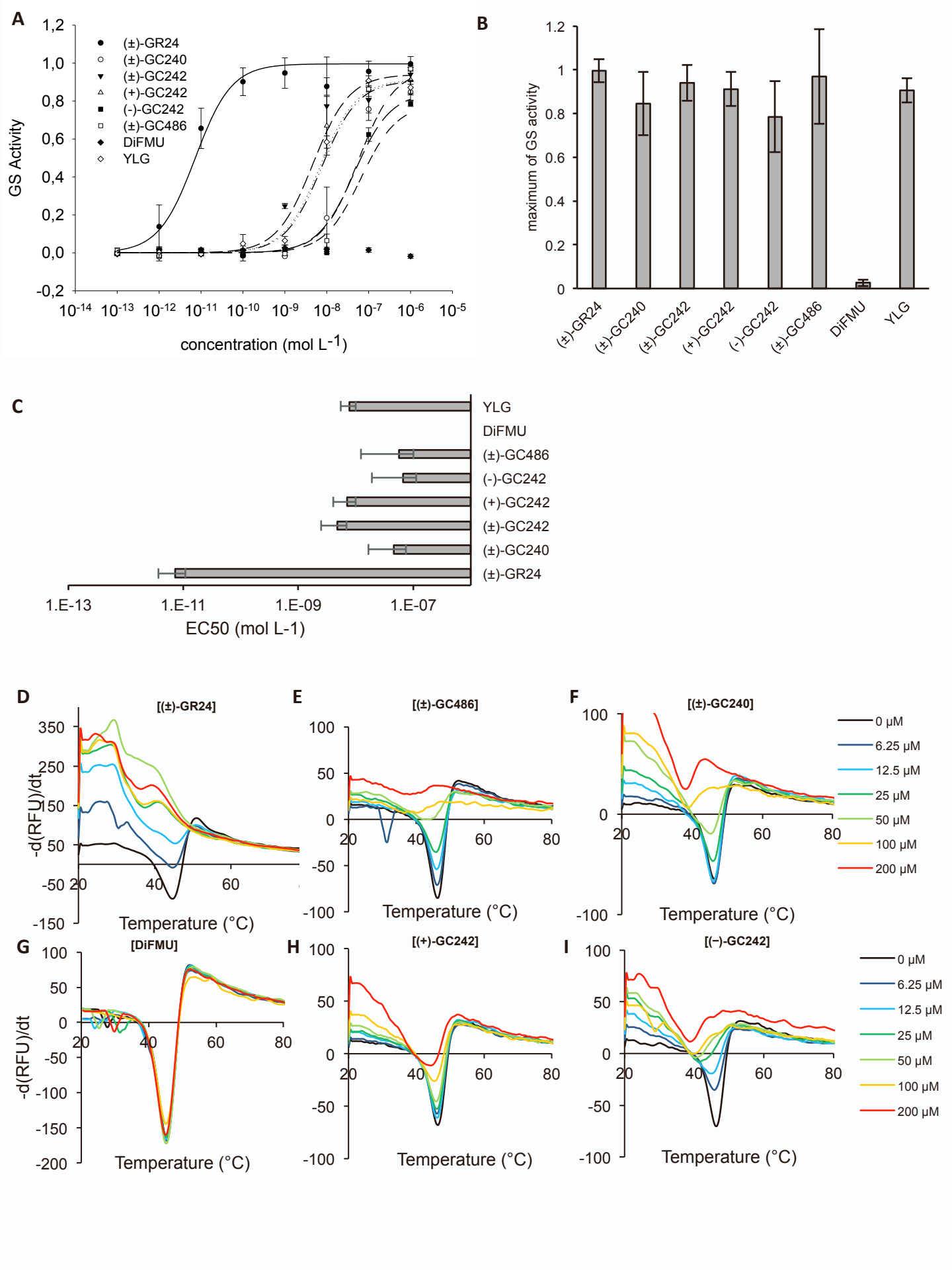
A
GS Activity
concentration (mol L-1)
(±)-GR24
(±)-GC240
(±)-GC242
(+)-GC242
(-)-GC242
(±)-GC486
DiFMU
YLG
B
maximum of GS activity
C
EC50 (mol L-1)
D
[(±)-GR24]
E
[(±)-GC486]
F
[(±)-GC240]
G
[DiFMU]
H
[(+)-GC242]
I
[(−)-GC242]
-d(RFU)/dt
Temperature (°C)
0 µM
6.25 µM
12.5 µM
25 µM
50 µM
100 µM
200 µM

Supplementary Figure 8. Germination assay on *P. ramosa* parasitic-plant seeds of various profluorescent ligands and biochemical analysis of the interaction between PrKAI2d3 and various ligands by DSF. (A) Dose response germination stimulation activities and modeled curves. **(B)** Maximum germination stimulant activity relative to (±)-GR24 (1 µM). **(C)** Half maximal effective concentration (EC_{50}) (mol L^{-1}). Data are indicated ± SE. **(D-I)** Melting temperature curves of PrKAI2d3 with (±)-GR24 **(D)**, (±)-GC486 **(E)**, (±)-GC240 **(F)**, DiFMU **(G)**, (+)-GC242 **(H),** and (−)-GC242 **(I)** at varying concentrations assessed by DSF. Each line represents the average protein melt curve for three technical replicates and the experiment was carried out twice.

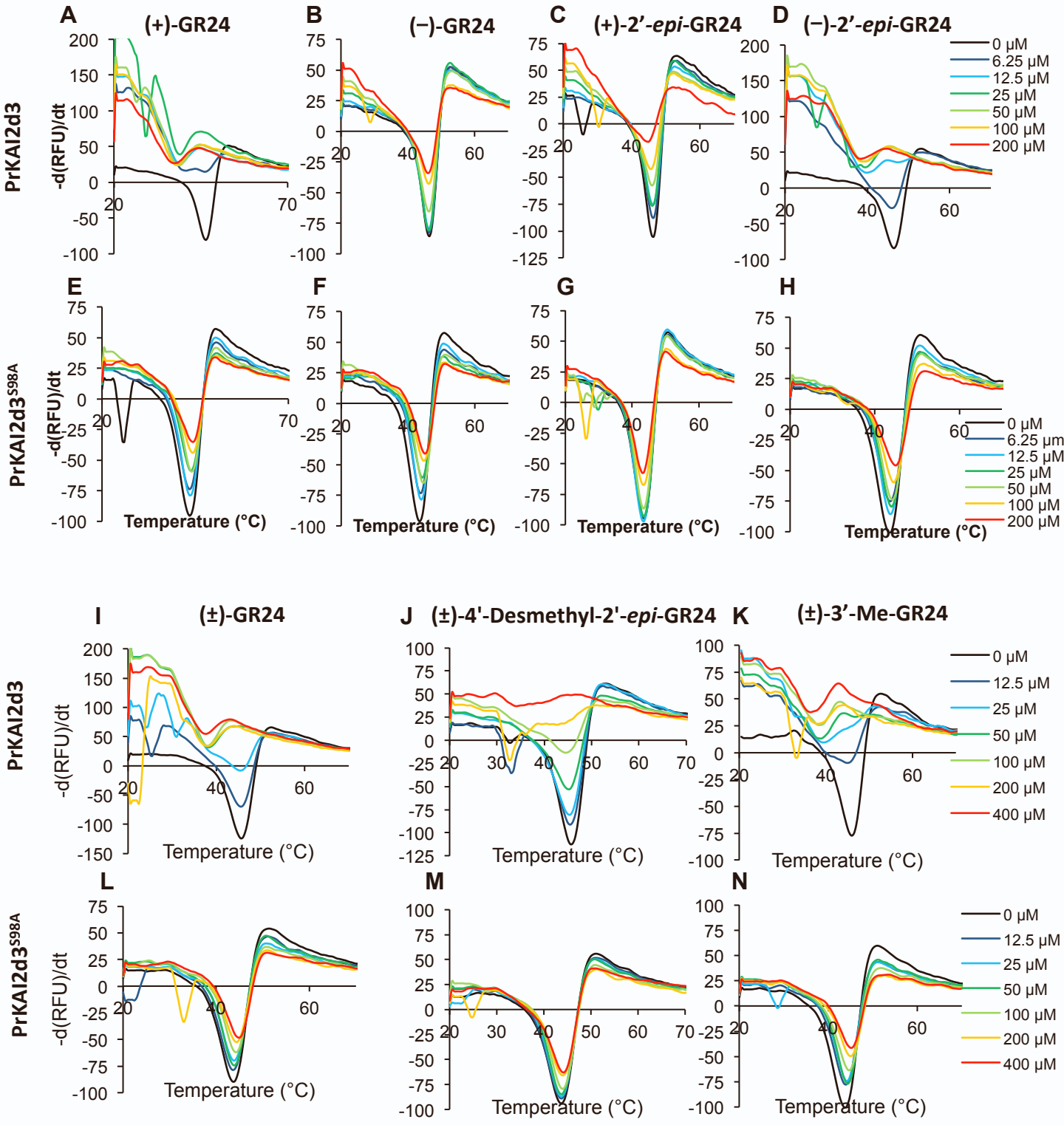

Supplementary Figure 9. Biochemical analysis of the interaction between PrKAI2d3 (A-D, I-K) or PrKAI2d3^{S98A} (E-H, L-N) and various ligands by DSF. Melting temperature curves of PrKAI2d3 or PrKAI2d3^{S98A} at 10 µM with (+)-GR24 **(A, E)**, (−)-GR24 **(B, F)**, (+)-2'-*epi*-GR24 **(C, G)**, (−)-2'-*epi*-GR24 **(D, H)**, (±)-GR24 **(I, L)**, (±)-4'-desmethyl-2'-*epi*-GR24 **(J, M)**, or (±)-3'-Me-GR24 **(K, N)** at varying concentrations assessed by DSF. Each line represents the average protein melt curve for three technical replicates and the experiment was carried out twice.

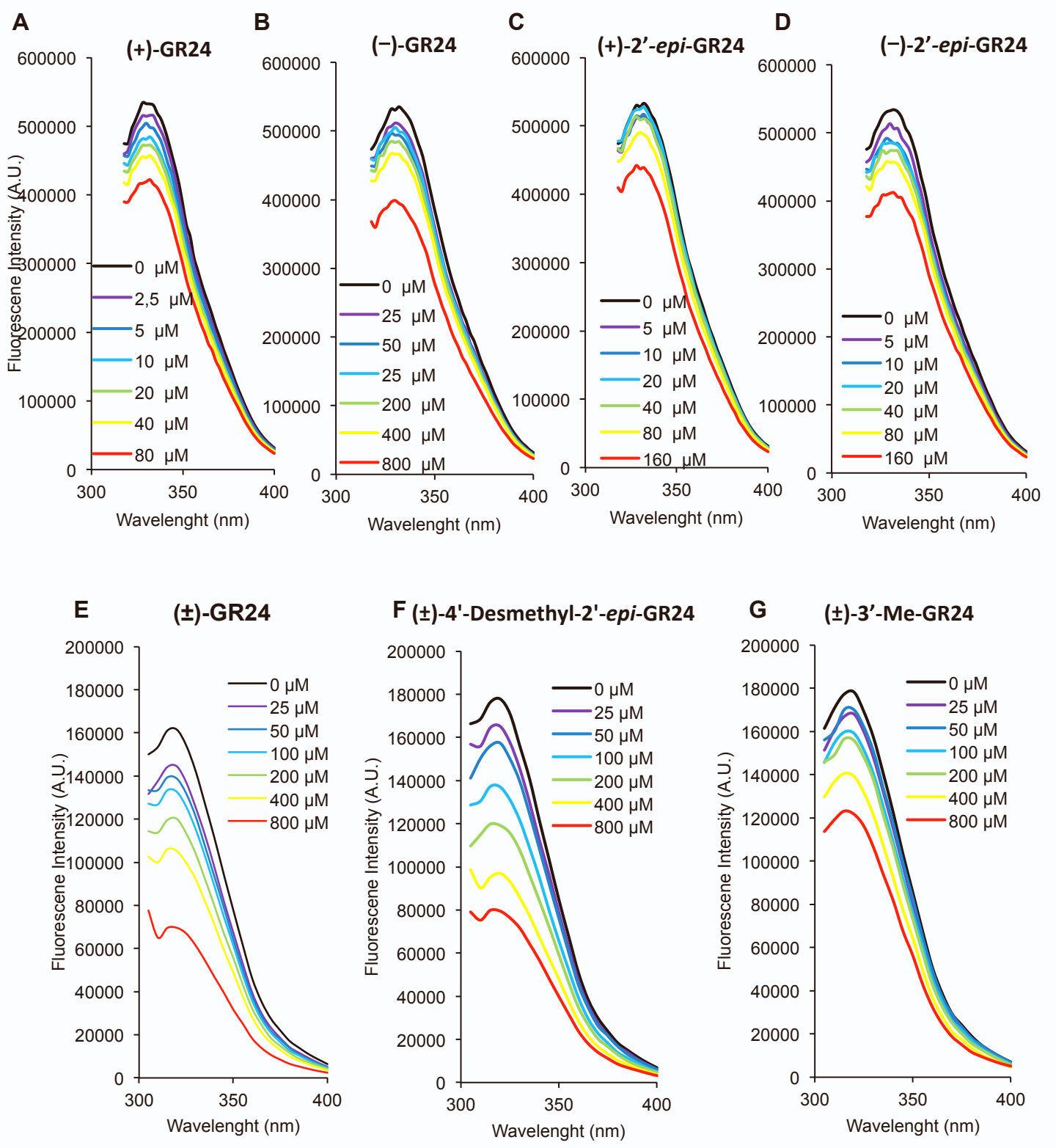

Supplementary Figure 10. Intrinsic tryptophan fluorescence of PrKAI2d3 in the presence of SL analogs. Changes in intrinsic fluorescence emission spectra of PrKAI2d3 in the presence of various concentrations of (+)-GR24 **(A)**, (−)-GR24 **(B)**, (+)-2'-*epi*-GR24 **(C)**, (−)-2'-*epi*-GR24 **(D)**, (±)-GR24 **(E)**, (±)-4'-desmethyl-2'-*epi*-GR24 **(F)**, or (±)-3'-Me-GR24 **(G)**. Proteins (10 µM) were incubated with increasing amounts of ligand (0–800 µM from top to bottom). The observed relative changes in intrinsic fluorescence were plotted as a function of the SL analog concentration, transformed to a saturation degree, and used to determine the apparent K_D values relevant to Figure 2**H,I**. The plots represent the mean of two replicates and the experiments were repeated at least three times. The analysis was done with GraphPad Prism 7.05 Software.

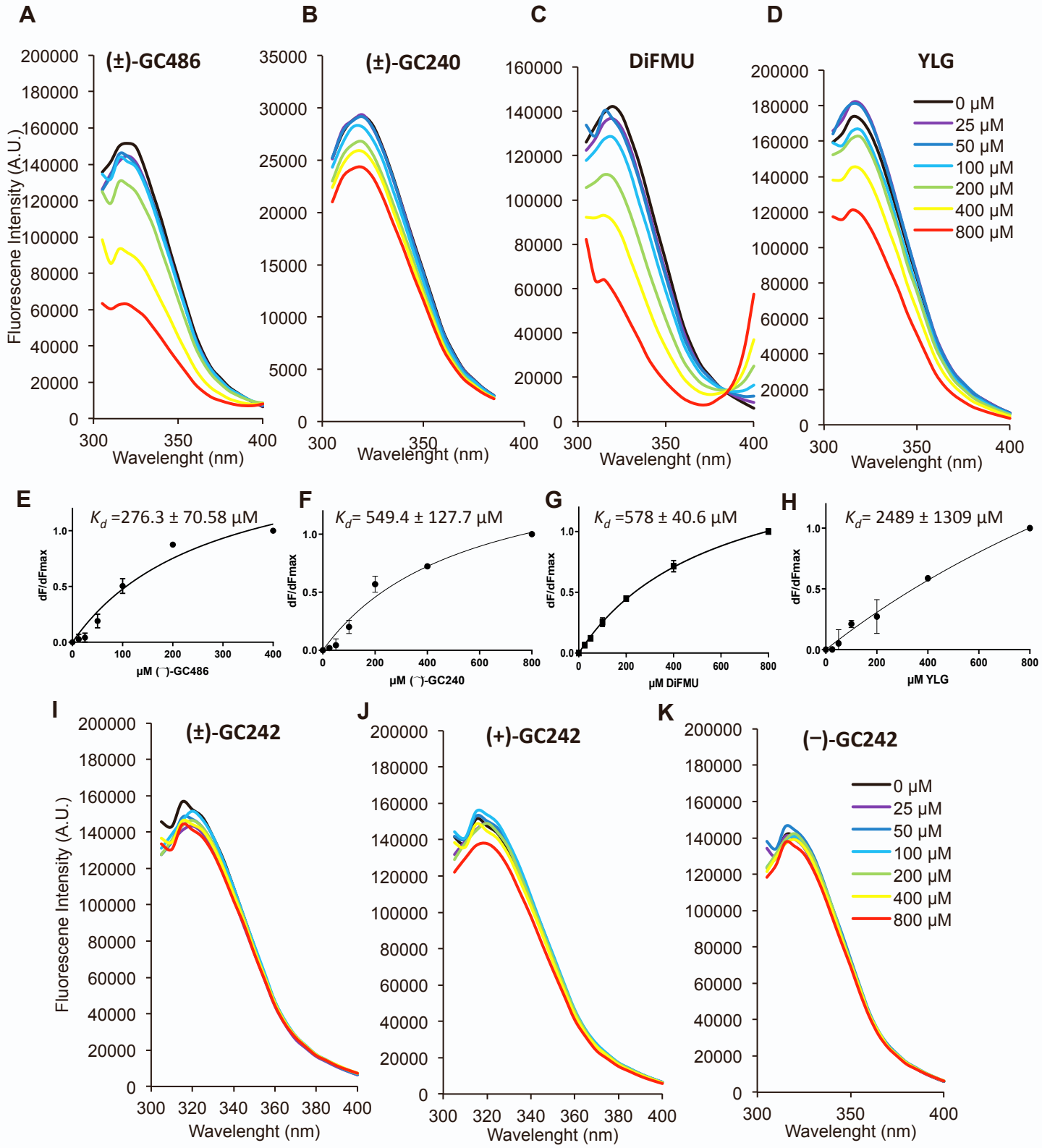
A
(±)-GC486
B
(±)-GC240
C
DiFMU
D
YLG
Fluorescene Intensity (A.U.)
Wavelenght (nm)
0 µM
25 µM
50 µM
100 µM
200 µM
400 µM
800 µM
E
K_d =276.3 ± 70.58 µM
F
K_d= 549.4 ± 127.7 µM
G
K_d =578 ± 40.6 µM
H
K_d= 2489 ± 1309 µM
dF/dFmax
µM (⁻)-GC486
µM (⁻)-GC240
µM DiFMU
µM YLG
I
(±)-GC242
J
(+)-GC242
K
(−)-GC242

Supplementary Figure 11. Intrinsic tryptophan fluorescence of PrKAI2d3 in the presence of profluorescent SL probes. Changes in intrinsic fluorescence emission spectra of PrKAI2d3 in the presence of various concentrations of (±)-GC486 (**A**), (±)-GC240 (**B**), DiFMU (**C**), YLG (**D**), (±)-GC242 (**I**), (+)-GC242 (**J**), or (−)-GC242 (**K**). Proteins (10 µM) were incubated with increasing amounts of ligand (0–800 µM from top to bottom). The observed relative changes in intrinsic fluorescence were plotted as a function of the SL analog concentration and transformed to saturation. Plots of fluorescence intensity *versus* (±)-GC486 (**E**), (±)-GC240 (**F**), DiFMU (**G**), and YLG (**H**) concentrations used to determine the apparent K_D values. The plots represent the mean of two replicates and the experiments were repeated at least three times. The analysis was done with GraphPad Prism 7.05 Software.

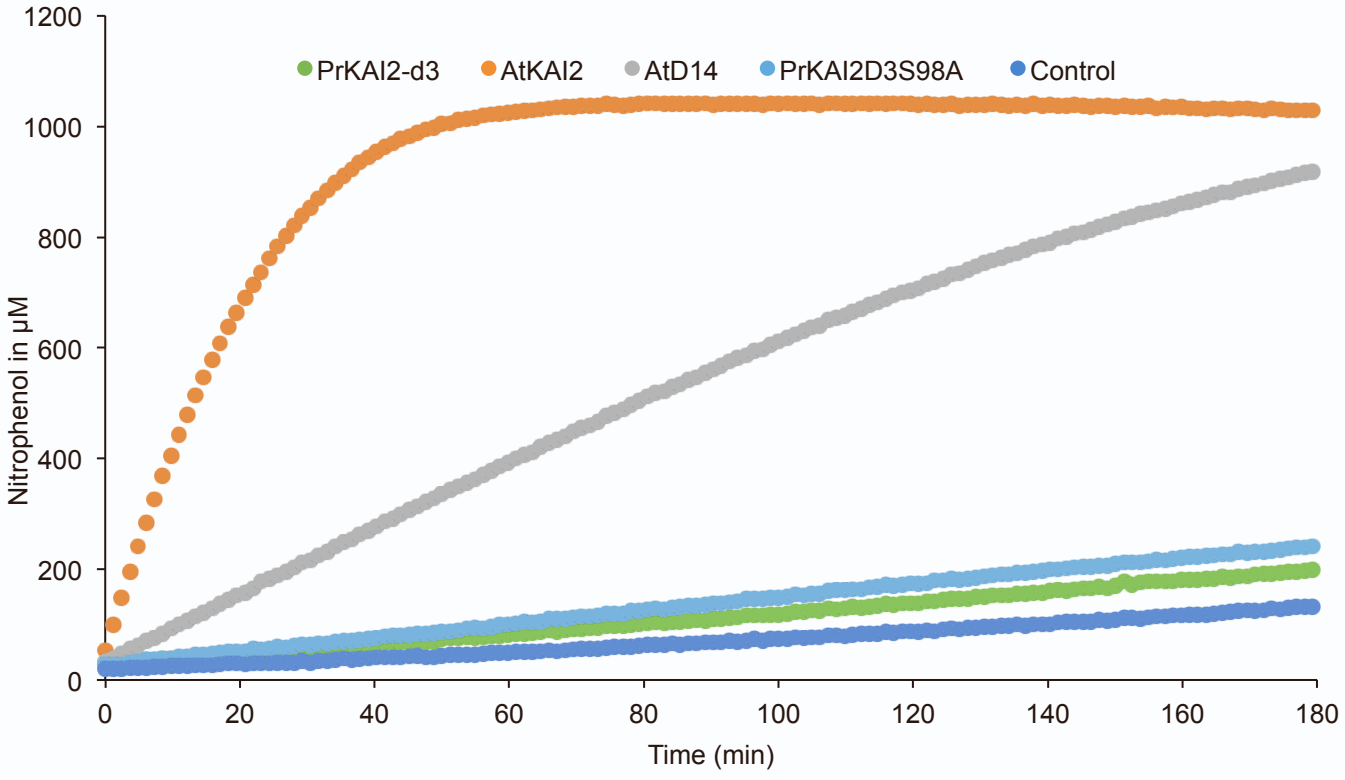

Supplementary Figure 12. PrKAI2d3 hydrolysis activity. Progress curves during the 4-nitrophenyl acetate (*p*-NPA) (1 mM) hydrolysis by PrKAI2d3, PrKAI2d3^{S98A}, AtKAI2, and AtD14 (4 µM). The *p*-NPA release was monitored (A_{405}) at 25 °C.

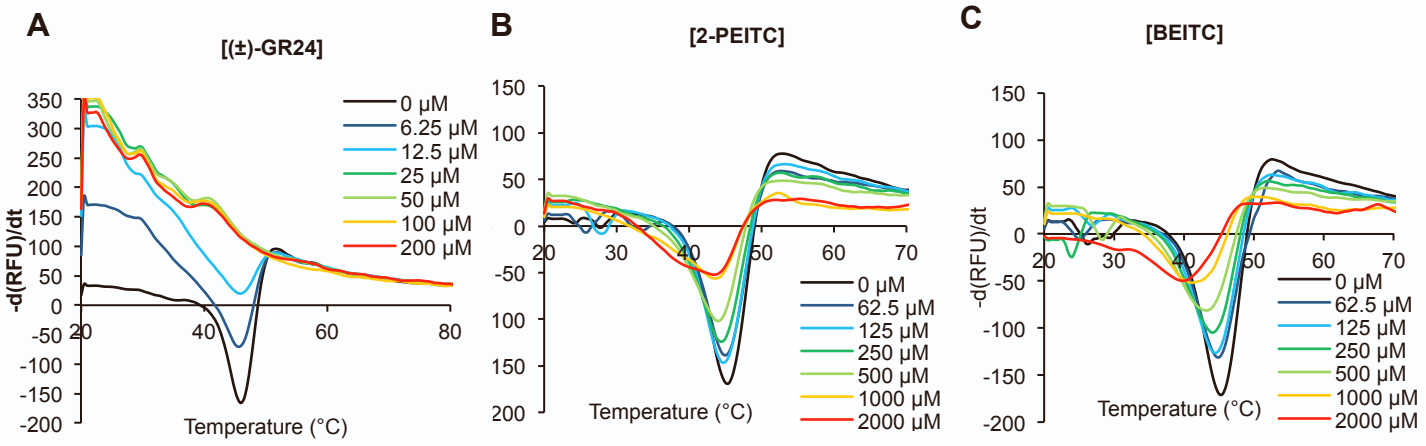

Supplementary Figure 13. Biochemical analysis of the interaction between PrKAI2d3 and ITCs by DSF. Melting temperature curves of PrKAI2d3 at 10 µM with (±)-GR24 **(A)**, 2-PEITC **(B)**, or BITC **(C)** at varying concentrations assessed by DSF. Each line represents the average protein melt curve for three technical replicates and the experiment was carried out twice.

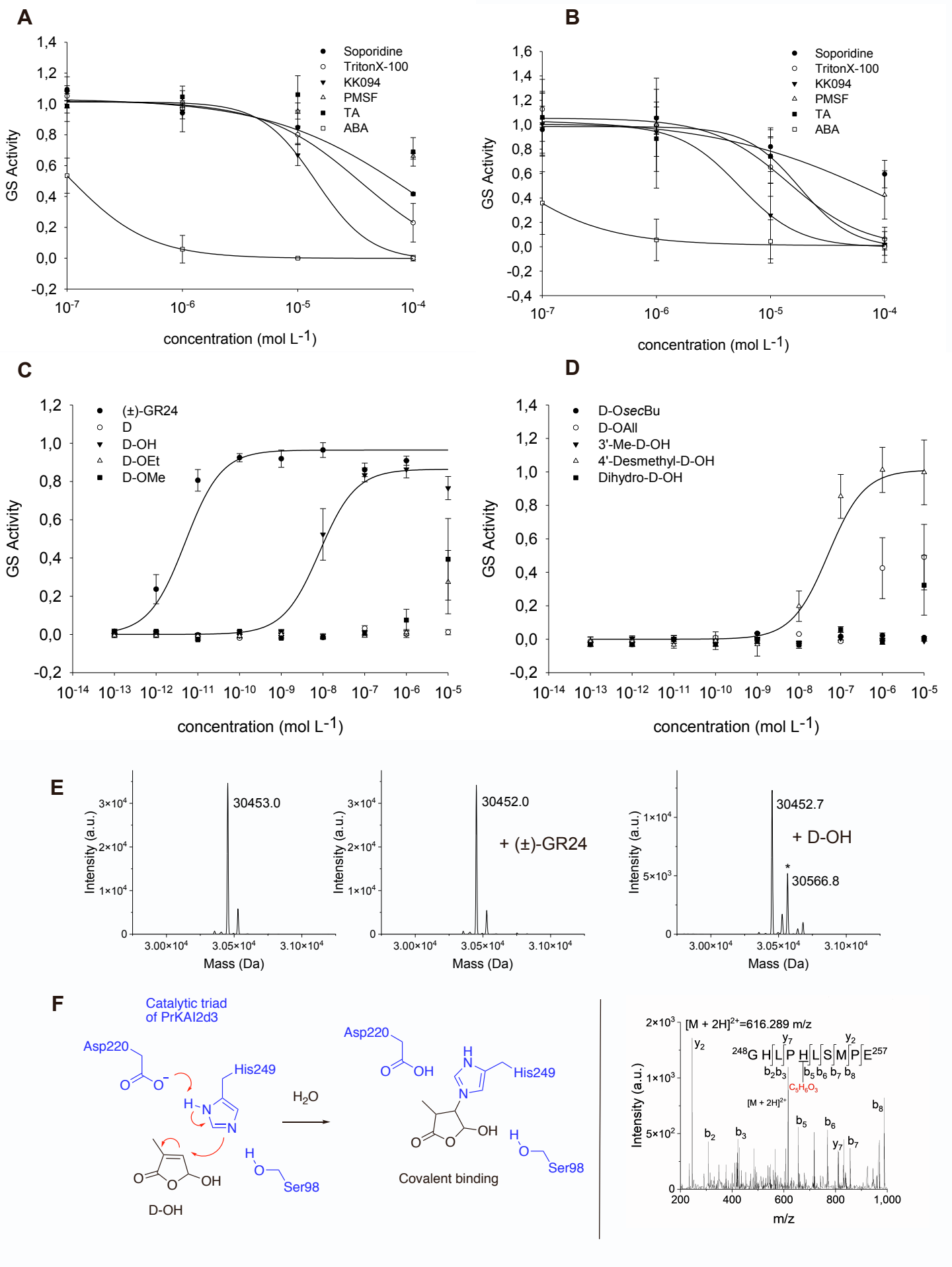
A
B
C
D
E
F
GS Activity
concentration (mol L-1)
Soporidine
TritonX-100
KK094
PMSF
TA
ABA
(±)-GR24
D
D-OH
D-OEt
D-OMe
D-OsecBu
D-OAll
3'-Me-D-OH
4'-Desmethyl-D-OH
Dihydro-D-OH
Intensity (a.u.)
Mass (Da)
30453.0
30452.0
+ (±)-GR24
30452.7
+ D-OH
30566.8
Catalytic triad
of PrKAI2d3
Asp220
His249
Ser98
H2O
D-OH
Covalent binding
[M + 2H]2+=616.289 m/z
m/z

Supplementary Figure 14. Germination inhibition by various chemicals and stimulation by D-analogs. Dose response germination stimulation (GS) activities with 10 nM (±)-GR24 **(A)** and 100 nM 2-PEITC (**B)** and modeled curves **(C**) and (**D)**. Maximum of germination stimulation activity relative to (±)-GR24 (1 µM). Data are indicated ± SE. **(E)** Putative adduct formed after incubation of D-OH with PrKAI2d3. **(F)** Deconvoluted electrospray mass spectra of PrKAI2d3^{S98A} alone, after addition of the D-OH ligand (10 mM) and after addition of the (±)-GR24 ligand (1 mM). The mass increments were measured for the PrKAI2d3^{S98A}-D-OH complex, 114.2 Da.

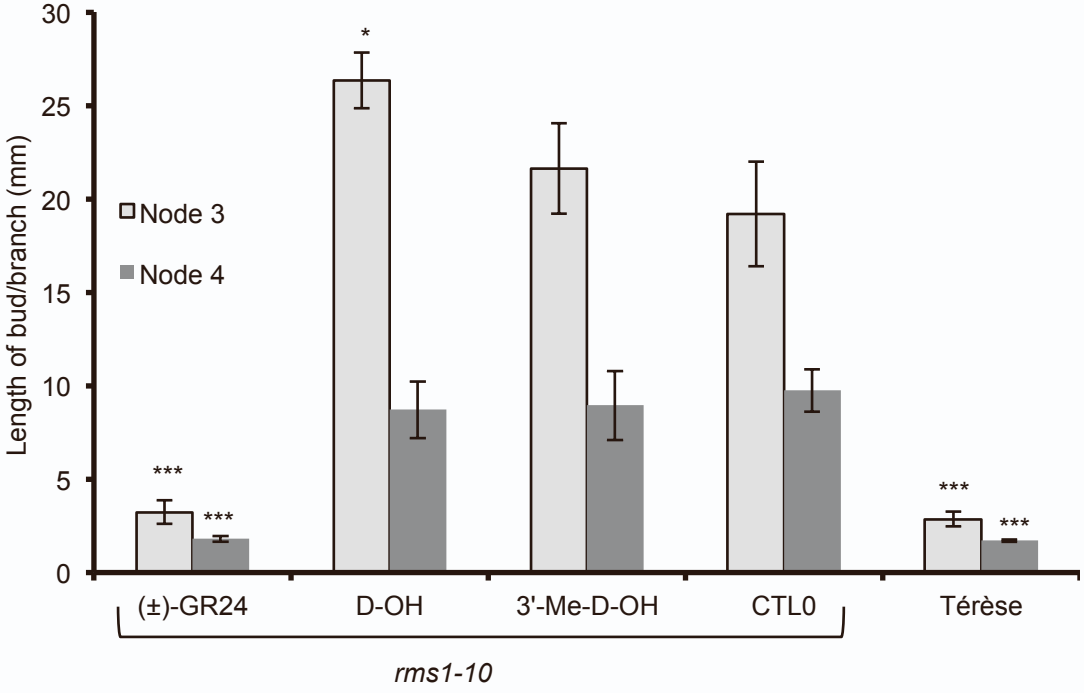

Supplementary Figure 15. Bud outgrowth inhibition activity assay for D derivatives after direct stem infusion. Data are means ± SE (*n* = 12), 8 days after treatment of the pea plants *rms1-10* and Térèse as control. **P* < 0.5, ****P* < 0.001, Kruskal-Wallis rank sum test, compared to control values (CTL0).

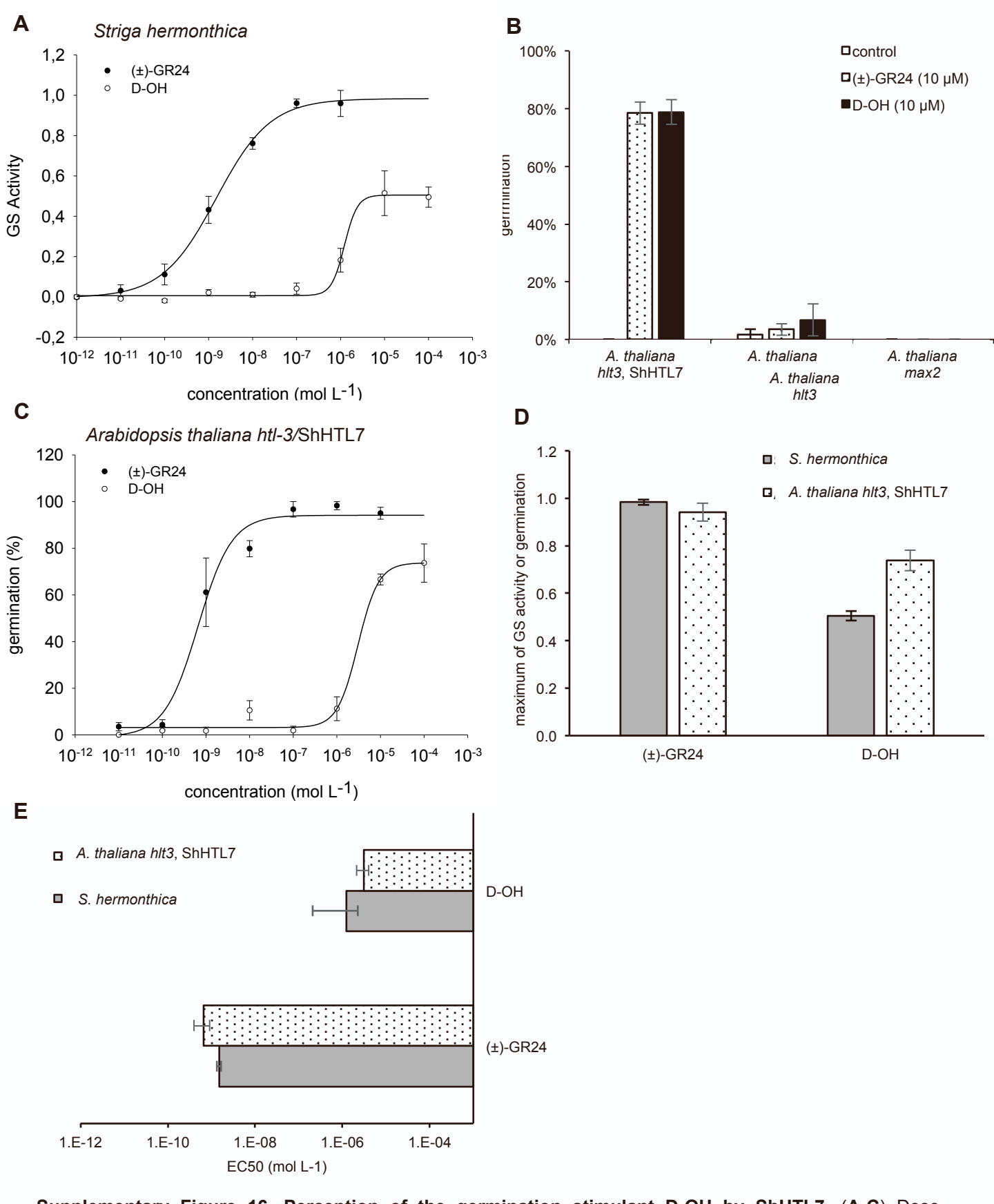

Supplementary Figure 16. Perception of the germination stimulant D-OH by ShHTL7. (**A-C**) Dose response germination stimulation activities and modeled curves of (±)-GR24 and D-OH on seeds of (**A**) *S. hermonthica*, (**C**) *A. thaliana htl-3*, ShHTL7 (34 °C, continuous light for *A. thaliana*). (**B**) Seed germination of *A thaliana htl-3*/ShHTL7, *htl-3* and *max2* with (±)-GR24 and D-OH (10 µM). (**D**) maximum germination stimulation activities and (e) EC_{50} (half maximal effective concentration). Data are indicated ± SE.

Supplementary Table 1. EC_{50} and maximum germination percentage of (+)-GR24, and (−)-GR24 and of (±)-GR24 and D-OH in *Arabidopsis* lines.

species	compound	EC50 (M)	SE	%max	SE
A. thaliana Col-0	(+)-GR24	nd		47%	4%
A. thaliana Col-0	(-)-GR24	1.6E-07	6.4E-08	80%	3%
A. thaliana htl-3	(+)-GR24	nd		9%	1%
A. thaliana htl-3	(-)-GR24	nd		10%	3%
A. thaliana htl-3/p35S::GFP-PrKAI2d3	(+)-GR24	5.9E-12	2.0E-11	75%	1%
A. thaliana htl-3/p35S::GFP-PrKAI2d3	(-)-GR24	4.9E-09	4.2E-09	76%	1%
Striga hermonthica	(±)-GR24	1.5E-09	1.6E-10	98%	1%
Striga hermonthica	D-OH	1.2E-06	1.0E-06	51%	2%
A. thaliana Col-0	(±)-GR24	1.5E-06	4.6E-07	85%	3%
*A. thaliana htl-3/*ShHTL7	(±)-GR24	6.6E-10	2.6E-10	94%	4%
*A. thaliana htl-3/*ShHTL7	D-OH	3.1E-06	9.4E-07	74%	4%

Supplementary Table 2. EC_{50} and maximum of germination stimulant activity of compounds for *P. ramosa*.

compound	EC50 (M)	SE	%max	SE
(+)-GR24	6.5E-12	3.0E-12	100%	5%
(−)-GR24	4.8E-09	2.3E-09	100%	9%
(+)-2'-*epi*-GR24	8.4E-10	2.8E-10	100%	6%
(−)-2'-*epi*-GR24	5.3E-12	2.6E-12	100%	5%
(±)-GR24	4.7E-12	2.6E-12	100%	5%
(±)-Desmethyl-GR24	4.5E-10	2.0E-10	92%	6%
(±)-4'-Desmethyl-2'-*epi*-GR24	9.2E-10	1.8E-10	98%	3%
(±)-3'-Me-GR24	2.6E-09	1.4E-09	95%	9%
(±)-GR24	7.3E-12	3.6E-12	100%	5%
(±)-GC240	4.6E-08	2.9E-08	85%	15%
(±)-GC242	4.7E-09	2.2E-09	94%	8%
(+)-GC242	7.0E-09	2.9E-09	91%	8%
(−)-GC242	6.6E-08	4.7E-08	79%	16%
(±)-GC486	5.7E-08	4.4E-08	97%	22%
DiFMU	nd	nd	3%	2%
YLG	7.7E-09	2.3E-09	91%	6%
(±)-GR24	5.3E-12	3.4E-12	100%	5%
2-PEITC	3.2E-08	2.0E-08	102%	15%
BITC	7.1E-08	2.7E-08	94%	11%
(±)-GR24	5.0E-12	3.1E-12	100%	5%
D-OH	8.3E-09	2.6E-09	86%	5%
D-OEt	nd		27%	14%
D-OMe	nd		39%	21%
D-OsecBu	nd		1%	1%
D-OAll	nd		49%	20%
3'-Me-D-OH	nd		0%	1%
4'-Desmethyl-D-OH	5.0E-08	2.1E-08	101%	8%
Dihydro-D-OEt	nd		32%	18%

Supplementary Table 3. IC_{50} and maximum of inhibition of putative inhibitors of PrKAI2d3 for *P. ramosa*.

	(±)-GR24 (10 nM)				2-PEITC (100 nM)			
compound	IC50(M)	SE	max. inh.	SE	IC50(M)	SE	max. inh.	SE
Soporidine	1.0E-04	8.5E-05	58%	1%	nd		40%	5%
TritonX-100	3.5E-05	6.0E-06	77%	13%	1.5E-05	4.1E-06	94%	6%
KK094	1.4E-05	4.5E-06	100%	2%	5.3E-06	1.3E-06	100%	3%
PMSF	nd		34%	2%	1.0E-04	9.0E-05	57%	20%
TA	nd		31%	9%	1.8E-05	9.5E-06	98%	14%
ABA	1.0E-07	9.4E-09	100%	1%	3.4E-08	2.1E-08	100%	7%

Supplementary Table 4. Oligonucleotides used.

Primer name	purpose	Sequence (5′—3′)	note
Cloning for protein expression			
PrKAI2d3_attb1_HRV3C	PrKAI2d3 coding sequence	ggggacaagtttgtacaaaaaagcaggct*ccctggaagtgctgttttcagggcccg*ATGAACATTAACAGAGACAT	Gene specifics sequences are capitalized Start and Stop codons are highlighted in bold Gateway recombination sites are underlined protease sites are in italic
PrKAI2d3_attb2	PrKAI2d3 coding sequence	ggggaccactttgtacaagaaagctgggtctcaTCAATTAGCATCTGC	
Cloning for complementation assay			
PrKAI2d3_attb2-F		ggggacagctttcttgtacaaagtggcaATGAACATTAACAGAGACATCGG	
PrKAI2d3_attb3-R		ggggacaactttgtataataaagttggATTAGCATCTGCAATATCATG	
PCR-Based mutagenesis			
PrKAI2d3_S98A-F		ctacgtcggccacgctctgtccgccat	
PrKAI2d3_S98A-R		atggcggacagagcgtggccgacgtag	
Q-PCR primer			
PrKAI2c_Fwd1		TGCCACATAATCCAGAGCATGAAG	
PrKAI2c_Rev1		CTAAGAAGCACAGGGACCACAAC	
PrKAI2d1_Fwd2		TGCGACCATTTCTCAAGGACG	
PrKAI2d1_Rev2		GAGATACCGCGACACTTTCACC	
PrKAI2d2_Fwd4		TGACGAATACGGAGGGATACGAAG	
PrKAI2d2_Rev4		TGCGAATCCCAACTGAAAGGAC	
PrKAI2d3_Fwd4		ACTGATCACGATCTCCACTTCCC	
PrKAI2d3_Rev4		CCATCCCCAACACCAATGACTC	
PrKAI2d4_Fwd2		TACGACCCGACATAGCCCTTAG	
PrKAI2d4_Rev2		TACGCCGATTTCGATGCCAC	
PrEF1a_Fwd		TTGCCGTGAAGGATCTGAAAC	

Supplementary Methods

Enzymatic degradation of GR24 isomers by purified proteins. The ligand (10 µM) was incubated without and with purified AtD14/AtKAI2/PrKAI2d3/PrKAI2d3^{S98A} (5 µM) for 150 min at 25ºC in 0.1 mL phosphate buffered saline (PBS; 100 mM Phosphate, pH 6.8, 150 mM NaCl) in the presence of (±)-1-indanol (100 M) as internal standard. The solutions were acidified to pH = 1 by addition of 2 µL trifluoroacetic acid (TFA) to quench the reaction and centrifugated (12 min, 12,000 tr/min). Thereafter, the samples were subjected to reverse-phase-ultra-performance liquid chromatography (RP-UPLC)-MS analyses by means of UPLC system equipped with a Photo Diode Array (PDA) and a Triple Quadrupole Detector (TQD) mass spectrometer (Acquity UPLC-TQD, Waters). RP-UPLC (HSS C_{18} column, 1.8 µm, 2.1 mm × 50 mm) with 0.1% (v/v) formic acid in CH_3CN and 0.1% (v/v) formic acid in water (aq. FA, 0.1%, v/v, pH 2.8) as eluents [10% CH_3CN, followed by linear gradient from 10% to 100% of CH_3CN (4 min)] at a flow rate of 0.6 mL min^{-1}. The detection was done by PDA and with the TQD mass spectrometer operated in Electrospray ionization-positive mode at 3.2 kV capillary voltage. To maximize the signal, the cone voltage and collision energy were optimized to 20 V and 12 eV, respectively. The collision gas was argon at a pressure maintained near 4.5 10^{-3} mBar.

Direct electrospray ionization (ESI)-MS under denaturing conditions. Mass spectrometry measurements were carried out with an electrospray quadrupole-time of flight (Q-TOF) mass spectrometer (Waters) equipped with the Nanomate device (Advion). The HD_A_384 chip (5 µm i.d. nozzle chip, flow rate range 100−500 nL/min) was calibrated before use. For the ESI−MS measurements, the Q-TOF instrument was operated in radio frequency quadrupole mode with the TOF data collected between *m/z* 400−2990. The collision energy was set to 10 eV and argon was used as collision gas. Mass spectra were acquired after denaturation of PrKAI2d3/PrKAI2d3^{S98A} [(50 µM in ammonium acetate buffer (50 mM, pH 6.8)] ± ligand in 50% (v/v) acetonitrile and 1% (v/v) formic acid. The Mass Lynx 4.1 (Waters) and Peakview 2.2 (AB Sciex) softwares were used for data acquisition and processing, respectively. Multiply-charged ions were deconvoluted by the MaxEnt algorithm (AB Sciex). The protein average masses were annotated in the spectra and the estimated mass accuracy was ± 2 Da. For the external calibration, NaI clusters (2 µg/µL, isopropanol/H_2O 50/50, Waters) were used in the acquisition *m/z* mass range.

Localization of the fixation site of ligands on PrKAI2d3. PrKAI2d3-ligand mixtures were incubated for 10 min prior overnight Glu-C proteolysis. Glu-C--generated peptide mixtures were analyzed by nanoLC-MS/MS with the Triple-TOF 4600 mass spectrometer (AB Sciex) coupled to the nanoRSLC UPLC system (Thermo Fisher Scientific) equipped with a trap column (Acclaim PepMap 100 C_{18}, 75 µm i.d. × 2 cm, 3 µm) and an analytical column (Acclaim PepMap RSLC C_{18}, 75 µm i.d. × 25 cm, 2 µm, 100 Å). Peptides were loaded at 5 µL/min with 0.05% (v/v) TFA in 5% (v/v) acetonitrile and separated at a flow rate of 300 nL/min with a 5% to 35% solvent B [0.1% (v/v) formic acid in 100% acetonitrile] gradient in 40 min with solvent A [0.1% (v/v) formic acid in water]. NanoLC-MS/MS experiments were conducted in a Data-Dependent acquisition method by selecting the 20 most intense precursors for collision-induced dissociation fragmentation with the Q1 quadrupole set at a low resolution for better sensitivity. Raw data were processed with the MS Data Converter tool (AB Sciex) for generation of .mgf data files and proteins were identified with the MASCOT search engine (Matrix Science) against the PrKAI2 sequence with oxidation of methionines and ligand-histidine adduct as variable modifications. Peptide and

fragment tolerance were set at 20 ppm and 0.05 Da, respectively. Only peptides were considered with a MASCOT ion score above the identity threshold (25) calculated at 1% false discovery rate.

Protein melting temperatures. For the Differential Scanning Fluorimetry (DSF) experiments a CFX96 Touch^{TM} Real-Time PCR Detection System (Bio-Rad) was used with excitation and emission wavelengths of 490 and 575 nm, respectively and Sypro Orange ($\lambda_{ex}/\lambda_{em}$: 470/570 nm; Life Technologies) as the reporter dye. Samples were heat-denatured with a linear 25 °C to 95 °C gradient at a rate of 1.3 °C per min after incubation at 25 °C for 30 min in the dark. The denaturation curve was obtained by means of the CFX manager™ software. Final reaction mixtures were prepared in triplicate in 96-well white microplates. Each reaction was carried out in 20-µL sample in PBS (100 mM phosphate, pH 6.8, 150 mM NaCl) containing 6 µg of protein (so that the final reactions contained 10 µM protein), 0 to X ligand concentrations in µM, 4% (v/v) DMSO, and 0.008 µL Sypro Orange. Plates were incubated in the dark for 30 min before analysis. In the control reaction, DMSO was added instead of the chemical solution. The experiments were repeated three times.

Plant material and growth conditions. Pea (*Pisum sativum*) branching mutant plants were derived from various cultivars after ethyl methanesulfonate (EMS) mutagenesis and had been described previously (Rameau et al., 1997). The *rms1-10* (M3T-884) mutant was obtained from the dwarf cv Térèse. Plants were grown in a greenhouse under long-day as described (Braun et al., 2012).
All *Arabidopsis thaliana* (L.) Heynh. mutant plants (Columbia-0 [Col-0] accession background) have been described previously: *htl-3* (ref. (Toh et al., 2014a; Toh et al., 2014b)), *Atd14-1/htl-3* (ref. (Toh et al., 2014a; Toh et al., 2014b)), and *htl-3* ShHTL7 (kind gift of P. McCourt). For overexpression of the green fluorescent protein (GFP) fusions of PrKAI2d3 and PrKAI2d3^{S98A}, transgenic *Arabidopsis* seeds were generated by the *Agrobacterium* floral dip method (Clough and Bent, 1998) with the *htl-3* mutant as the background accession. Transgenic seeds were selected based on the antibiotic resistance and GFP fluorescence.

Pea shoot-branching assay. The compounds to be tested were applied by vascular supply. The control was the treatment with 0.1% dimethylsulfoxide (DMSO) only. Twelve plants were sown per treatment in trays and generally 10 days after sowing the axillary bud at node 3 was treated. Compounds in DMSO solution were diluted in water to the indicated concentrations for a treatment with 0.1% (v/v) DMSO. The branches at nodes 1 and 2 were removed to encourage the outgrowth of axillary buds at the nodes above. Nodes were numbered acropetally from the first scale leaf as node 1 and cotyledonary node as node 0. Bud growth at nodes 3 and 4 was measured with digital callipers 8 to 10 days after treatment. Plants with damaged main shoot apex or with a dead white treated-bud were discarded from the analysis. The SL-deficient *rms1-10* pea mutant was used for all experiments.

General experimental procedures for synthetic chemistry

All non-aqueous reactions were run under an inert atmosphere (argon), by using standard techniques for manipulating air-sensitive compounds. All glassware was stored in the oven and/or was flame-dried prior to use. Anhydrous solvents were obtained by filtration through drying columns. Analytical thin-layer chromatographies (TLC) were performed on plates precoated with silica gel layers. Compounds were visualized by one or more of the following methods: (1) illumination with a short wavelength UV lamp (i.e., λ = 254 nm), (2) spray with

a $KMnO_4$ solution in H_2O. Flash column chromatography was performed using 40-63 mesh silica. Nuclear magnetic resonance spectra (^1H; ^{13}C NMR) were recorded respectively at [500; 125] MHz on a Bruker DPX 500 spectrometer. For the ^1H spectra, data are reported as follows: chemical shift, multiplicity (s = singlet, d = doublet, t = triplet, q = quartet, m = multiplet, bs = broad singulet, coupling constant in Hz and integration. IR spectra are reported in reciprocal centimeters (cm^{-1}). Mass spectra (MS) and high-resolution mass spectra (HRMS) were determined by electrospray ionization (ESI) coupled to a time-of-flight analyser (Waters LCT Premier XE).

Preparation of GR24 isomers, probes, and other ligands. For general experimental procedures, see the Supplementary Methods. (±)-2'-*epi*-GR24 and (±)-GR24 were prepared as described (Mangnus et al., 1992) and (±)-4'-desmethyl-GR24, (±)-2'-*epi*-4'-desmethyl-GR24, and (±)-3'-Me-GR24 as described (Boyer et al., 2012). (+)-GR24, (−)-GR24, (+)-2'-*epi*-GR24, and (−)-2'-*epi*-GR24 were separated from (±)-2'-*epi*-GR24 and (±)-GR24 by chiral supercritical fluid chromatography as described (de Saint Germain et al., 2016; de Saint Germain et al., 2019). (±)-GR24 was purified by semi-preparative HPLC by means of a Interchim puriFlash® 4250 instrument, combined with a fraction collector with integrated ELSD, a PDA and a Phenomenex Luna C18, 250 × 21.2 mm, 5-µm column (H_2O/CH_3CN: 6/4) or Interchim Uptisphere Strategy SI, 250 × 21.2 mm, 5-µm column (Heptane/EtOAc: 1/1). 2-Phenethyl isothiocyanate (2-PEITC), benzylisothiocyanate (BEITC), DiFMU, *para*-nitrophenyl acetate (*p*-NPA), Yoshimulactone Green (YLG), abscisic acid (ABA), tolfenamic acid (Hamiaux et al., 2018) (TA), TritonX-100 (Shahul Hameed et al., 2018) and phenylmethylsulfonyl fluoride (PMSF) are commercially available. KK094 (Nakamura et al., 2019) and soporidine (Holbrook-Smith et al., 2016) were kindly provided by T. Asami and P. McCourt (University of Toronto), respectively. Probes (GC486, GC240, and GC242) were prepared as described (de Saint Germain et al., 2016).

Preparation of GR24 isomers

(±)-2'-*epi*-GR24 and (±)-GR24 were prepared according to described procedures (Mangnus et al., 1992). ((+)-GR24, (−)-GR24, (+)-2'-*epi*-GR24, (−)-2'-*epi*-GR24 were separated from (±)-2'-*epi*-GR24 and (±)-GR24 by chiral supercritical fluid chromatography as described in (de Saint Germain et al., 2016). (±)-GR24 can be purified by semi-preparative HPLC. Semi-preparative HPLC was performed using a Interchim puriFlash® 4250 instrument, combined with a fraction collector with integrated ELSD, a PDA and a Phenomenex Luna C18, 250 × 21.2 mm, 5 µm column (H_2O/CH_3CN : 6 /4) or Interchim Uptisphere Strategy SI, 250 × 21.2 mm, 5 µm column (Heptane/EtOAc : 1 /1).

Preparations of D-OH and analogs

(±)-D-OH was prepared according to Fell & Harbridge (Fell and Harbridge, 1990). (±)-3'-Methyl-D-OH was prepared according to Canévet & Graff (Canévet and Graff, 1978).

Preparation of (±)-D-OEt (Bayer et al., 2016; Wigchert and Zwanenburg, 1999) **by a modification of the Bayer et al. procedure** (Bayer et al., 2016)

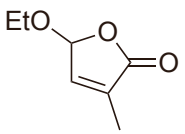

To a 0 °C solution of $TiCl_4$ (16.5 mL, 150 mmol) in anhydrous CH_2Cl_2 (212 mL) was added dropwise under argon a mixture of ethyl pyruvate (16.5 mL, 150 mmol) and vinyl acetate (16.5 mL, 150 mmol) in anhydrous CH_2Cl_2 (106 mL). When addition is complete, the suspension was further stirred for 2 hours at 0 °C. The reaction mixture was quenched with H_2O (140 mL). The aqueous solution was extracted with CH_2Cl_2 (2 × 100 mL). The combined organic layers were washed with H_2O (100 mL), brine (100 mL), dried (Na_2SO_4), filtered and evaporated under

reduced pressure. The residue (30 g) was diluted in EtOH (345 mL), AcOH (17 mL), conc. HCl (17 mL) and stirred under reflux for 4 hours. EtOH was removed by distillation and the cooled residue was extracted with EtOAc (3 × 150 mL). The combined organic layers were washed with brine, dried (Na_2SO_4), filtered and evaporated under reduced pressure. The residue was distilled (120-130 °C) with Kugelrohr to give (±)-D-OEt (Wigchert and Zwanenburg, 1999) as a pale yellow liquid (9.3 g, 65.5 mmol, 44%).

Preparation of (±)-D-OMe (Chapleo et al., 1976)

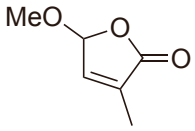

A mixture of (±)-D-O-Et (1.00 g, 7.04 mmol) and *para*-toluene sulfonic acid (250 mg, 1.31 mmol) in MeOH (44 mL) was stirred for 48 h at room temperature. MeOH was removed under reduced pressure and the residue was diluted with EtOAc (50 mL). The organic solution was washed with a $NaHCO_3$ saturated aqueous solution, brine, dried ($MgSO_4$), filtered and evaporated under reduced pressure. The residue was distilled (1 mm Hg, 70-110 °C) with Kugelrohr to give (±)-D-OMe (Chapleo et al., 1976) as a colourless liquid (0.81 g, 6.33 mmol, 90%).

Preparation of (±)-Dihydro-D-OEt

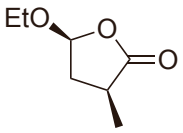

A solution of (±)-D-OEt (Wigchert and Zwanenburg, 1999) (429 mg, 3.02 mmol) and 10% Pd/C (170 mg) in EtOAc (45 mL) was stirred under H_2 atmosphere for 75 min at room temperature, flushed with argon and filtered on Celite. The resultant solution was evaporated under reduced pressure and distilled (1 mm Hg, 80-90 °C) with Kugelrohr to give (±)-Dihydro-D-OEt (Redon et al., 2008) as a colourless liquid (266 mg, 1.84 mmol, 61%).

Preparation of (±)-Dihydro-D-O*sec*-Bu

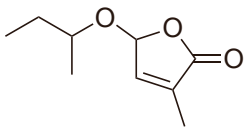

A mixture of (±)-D-O-Et (2.02 g, 14.02 mmol) and *para*-toluene sulfonic acid (503 mg) in *sec*-BuOH (40 mL) was stirred for 3 h at reflux. *sec*-BuOH was removed under reduced pressure and the residue was diluted with EtOAc (200 mL). The organic solution was washed with a 5% $NaHCO_3$ aqueous solution (2 × 50 mL), dried ($MgSO_4$), filtered and evaporated under reduced pressure. The residue was distilled (1 mm Hg, 70-110 °C) with Kugelrohr to give (±)-D-O*sec*-Bu as a colourless liquid (1.11 g, 6.52 mmol, 46%). Mixture of 2 diastereomers (1:1). ^{1}H NMR ($CDCl_3$, 300 MHz): δ (ppm) 0.87 (t, J = 7.5 Hz, 3H), 0.90 (t, J = 7.5 Hz, 3H), 1.19 (d, J = 6.0 Hz, 3H), 1.23 (d, J = 6.0 Hz, 3H), 1.44-1.64 (m, 4H), 1.89-1.91 (m, 6H), 3.75-3.85 (m, 2H), 5.81-5.83 (m, 1H), 5.83-5.86 (m, 1H), 6.73-6.76 (m, 2H). ^{13}C NMR ($CDCl_3$, 75 MHz): δ (ppm) 9.7 (CH_3), 9.8 (CH_3), 10.72 (CH_3), 10.76 (CH_3), 19.4 (CH_3), 20.9 (CH_3), 29.5 (CH_2), 29.9 (CH_2), 77.5 (CH), 77.9 (CH), 100.2 (CH), 101.7 (CH), 133.9 (2C), 143.3 (CH), 143.5 (CH), 172.28 (C), 172.30 (C). HRMS (ESI): Calculated for $C_9H_{15}O_3$ $[M + H]^+$: 171.1021. Found: 171.1019.

Preparation of (±)-Dihydro-D-OAll

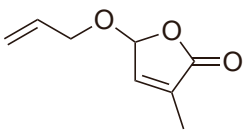

A mixture of (±)-D-O-Et (1.01 g, 7.13 mmol) and *para*-toluene sulfonic acid (250 mg, 1.31 mmol) in allylic alcohol (40 mL) was stirred for 24 h at room temperature. Allylic alcohol was removed under reduced pressure and the residue was diluted with EtOAc (100 mL). The organic solution was washed with a 5% $NaHCO_3$ aqueous solution (2 × 50 mL), dried ($MgSO_4$), filtered and evaporated under reduced pressure. The residue was distilled (20 mm Hg, 90 °C) with Kugelrohr to give (±)-D-OAll as a colourless liquid (719 mg, 4.66 mmol, 65%). ^{1}H NMR ($CDCl_3$, 300 MHz): δ (ppm) 1.90 (s, 3H), 4.16 (dd, J = 12.5, 6.5 Hz, 1H), 4.32 (dd, J = 12.5, 5.5 Hz, 1H), 5.22 (d, J = 10.5 Hz, 1H), 5.30 (dd, J = 17.0, 3.0 Hz,

1H), 5.79-5.81 (bs, 1H), 5.82-5.95 (m, 1H), 6.78-6.79 (bs, 1H). ^{13}C NMR ($CDCl_3$, 75 MHz): δ (ppm) 10.7 (CH_3), 70.8 (CH_2), 100.7 (CH), 119.0 (CH_2), 133.0 (CH), 134.3 (C), 143.0 (CH), 172.0 (C). IR (film): ν (cm^{-1}) 3085, 2983, 2928, 1764, 1668, 1649. HRMS (ESI): Calculated for $C_8H_{11}O_3$ $[M + H]^+$: 155.0708. Found: 155.0703.

Preparation of (±)-4'-desmethyl-D-OH

To a solution of (±)-4'-desmethyl-D-Br (Wolff and Hoffmann, 1988) (200 mg, 1.23 mmol) was added an aqueous solution of KOH (2 mL, 2 M). The resultant mixture was stirred at room temperature for 2 h, neutralized with an aqueous solution of HCl (1 M) and extracted with EtOAc (3 × 15 mL). The combined organic layers were dried (Na_2SO_4), filtered and evaporated under reduced pressure. The residue was chromatographied on silica gel (Heptane/ EtOAc 100:0 to 1:1) to give (±)-4'-desmethyl-D-OH (Byun et al., 2018) as a white solid (45 mg, 37%).

References

Bayer, T.S., Davidson, E.A., and Hleba, Y. (2016). Methods for hydraulic enhancement of crops. PCT/US2016/029080.

Boyer, F.-D., de Saint Germain, A., Pillot, J.-P., Pouvreau, J.-B., Chen, V.X., Ramos, S., Stévenin, A., Simier, P., Delavault, P., Beau, J.-M., et al. (2012). Structure-Activity Relationship Studies of Strigolactone-Related Molecules for Branching Inhibition in Garden Pea: Molecule Design for Shoot Branching. Plant Physiol. 159:1524-1544.

Braun, N., de Saint Germain, A., Pillot, J.P., Boutet-Mercey, S., Dalmais, M., Antoniadi, I., Li, X., Maia-Grondard, A., Le Signor, C., Bouteiller, N., et al. (2012). The pea TCP transcription factor PsBRC1 acts downstream of Strigolactones to control shoot branching. Plant Physiol. 158:225-238.

Byun, J., Huang, W., Wang, D., Li, R., and Zhang, K.A.I. (2018). CO2 -Triggered Switchable Hydrophilicity of a Heterogeneous Conjugated Polymer Photocatalyst for Enhanced Catalytic Activity in Water. Angew. Chem. Int. Ed. 57:2967-2971.

Canévet, J.C., and Graff, Y. (1978). Réactions de Friedel-Crafts de dérivés aromatiques sur des composés dicarbonylés-1,4éthyléniques-2,3.II Alkylations par quelques hydroxy-5 ou chloro-5 dihydro-2,5 furannones-2. Nouvelle méthode de synthèse des acides 1H-indènecarboxyliques-1. Tetrahedron 34:1935-1942.

Chapleo, C.B., Svanholt, K.L., Martin, R., and Dreiding, A.S. (1976). Synthesis of Bromo-substituted 2-Buten- and 2-Penten-4-olides. Helv. Chim. Acta 59:100-107.

Clough, S.J., and Bent, A.F. (1998). Floral dip: a simplified method for Agrobacterium-mediated transformation of *Arabidopsis thaliana*. Plant J. 16:735-743.

de Saint Germain, A., Clavé, G., Badet-Denisot, M.-A., Pillot, J.-P., Cornu, D., Le Caer, J.-P., Burger, M., Pelissier, F., Retailleau, P., Turnbull, C., et al. (2016). An histidine covalent receptor and butenolide complex mediates strigolactone perception. Nat. Chem. Biol. 12:787-794.

de Saint Germain, A., Retailleau, P., Norsikian, S., Servajean, V., Pelissier, F., Steinmetz, V., Pillot, J.-P., Rochange, S., Pouvreau, J.-B., and Boyer, F.-D. (2019). Contalactone, a contaminant formed during chemical synthesis of the strigolactone reference GR24 is also a strigolactone mimic. Phytochemistry 168:112112.

Fell, S.C.M., and Harbridge, J.B. (1990). 2,5-dimethoxy-2,5-dihydrofuran: A convenient synthon for a novel mono-protected glyoxal; synthesis of 4-hydroxybutenolides. Tetrahedron Lett. 31:4227-4228.

Hamiaux, C., Drummond, R.S.M., Luo, Z.W., Lee, H.W., Sharma, P., Janssen, B.J., Perry, N.B., Denny, W.A., and Snowden, K.C. (2018). Inhibition of strigolactone receptors

by N-phenylanthranilic acid derivatives: Structural and functional insights. J. Biol. Chem. 293:6530-6543.
Holbrook-Smith, D., Toh, S., Tsuchiya, Y., and McCourt, P. (2016). Small-molecule antagonists of germination of the parasitic plant *Striga hermonthica*. Nat. Chem. Biol. 12:724-729.
Mangnus, E.M., Dommerholt, F.J., Dejong, R.L.P., and Zwanenburg, B. (1992). Improved Synthesis of Strigol Analog GR24 and Evaluation of the Biological-Activity of Its Diastereomers. J. Agric. Food. Chem. 40:1230-1235.
Nakamura, H., Hirabayashi, K., Miyakawa, T., Kikuzato, K., Hu, W., Xu, Y., Jiang, K., Takahashi, I., Niiyama, R., Dohmae, N., et al. (2019). Triazole Ureas Covalently Bind to Strigolactone Receptor and Antagonize Strigolactone Responses. Mol. Plant 12:44-58.
Rameau, C., Bodelin C, Cadier D, Grandjean O, Miard F, and Murfet IC. (1997). New *ramosus* mutants at loci *Rms1*, *Rms3* and *Rms4* resulting from the mutation breeding program at Versailles. Pisum Genetics 29:7-12.
Redon, S., Pannecoucke, X., Franck, X., and Outurquin, F. (2008). Synthesis and oxidative rearrangement of selenenylated dihydropyrans. Org. Biomol. Chem. 6:1260-1267.
Shahul Hameed, U., Haider, I., Jamil, M., Kountche, B.A., Guo, X., Zarban, R.A., Kim, D., Al-Babili, S., and Arold, S.T. (2018). Structural basis for specific inhibition of the highly sensitive ShHTL7 receptor. EMBO Rep. 19:e45619.
Toh, S., Holbrook-Smith, D., Stokes, M.E., Tsuchiya, Y., and McCourt, P. (2014a). Detection of Parasitic Plant Suicide Germination Compounds Using a High-Throughput Arabidopsis HTL/KAI2 Strigolactone Perception System. Chem. Biol. 21:988-998.
Toh, S., Holbrook-Smith, D., Stokes, Michael E., Tsuchiya, Y., and McCourt, P. (2014b). Erratum. Chem. Biol. 21:1253.
Wigchert, S.C.M., and Zwanenburg, B. (1999). A critical account on the reception of Striga seed germination. J. Agric. Food. Chem. 47:1320-1325.
Wolff, S., and Hoffmann, H.M.R. (1988). Aflatoxins revisited - convergent synthesis of the ABC-moiety. Synthesis:760-763.